Zoology 117 (2014) 19–27

Contents lists available at ScienceDirect

Zoology

journal homepage: www.elsevier.com/locate/zool

Built for speed: strain in the cartilaginous vertebral columns of sharks☆

M.E. Porter[a,b,*], Candido Diaz Jr.[b,f], Joshua J. Sturm[b,e], Sindre Grotmol[c], A.P. Summers[d], John H. Long Jr.[b]

[a] Department of Biological Sciences, Florida Atlantic University, 777 Glades Road, Boca Raton, FL 33431, USA
[b] Department of Biology, Vassar College, 124 Raymond Avenue, Poughkeepsie, NY 12603, USA
[c] Department of Biology, University of Bergen, Thormøhlensgt. 53 A/B, 5020 Bergen, Norway
[d] Friday Harbor Laboratories, University of Washington, 620 University Road, Friday Harbor, WA 98250, USA
[e] University of Pittsburgh, 4200 Fifth Avenue, Pittsburgh, PA 15213, USA
[f] Department of Biology, University of Akron, 302 E Buchtel Avenue, Akron, OH 44304, USA

ARTICLE INFO

Article history:
Received 18 August 2013
Received in revised form 22 October 2013
Accepted 25 October 2013
Available online 5 December 2013

Keywords:
Cartilaginous fishes
Intervertebral joints
Vertebral column strain
Elastic energy
Locomotion

ABSTRACT

In most bony fishes vertebral column strain during locomotion is almost exclusively in the intervertebral joints, and when these joints move there is the potential to store and release strain energy. Since cartilaginous fishes have poorly mineralized vertebral centra, we tested whether the vertebral bodies undergo substantial strain and thus may be sites of energy storage during locomotion. We measured axial strains of the intervertebral joints and vertebrae in vivo and ex vivo to characterize the dynamic behavior of the vertebral column. We used sonomicrometry to directly measure in vivo and in situ strains of intervertebral joints and vertebrae of *Squalus acanthias* swimming in a flume. For ex vivo measurements, we used a materials testing system to dynamically bend segments of vertebral column at frequencies ranging from 0.25 to 1.00 Hz and a range of physiologically relevant curvatures, which were determined using a kinematic analysis. The vertebral centra of *S. acanthias* undergo strain during in vivo volitional movements as well as in situ passive movements. Moreover, when isolated segments of vertebral column were tested during mechanical bending, we measured the same magnitudes of strain. These data support our hypothesis that vertebral column strain in lateral bending is not limited to the intervertebral joints. In histological sections, we found that the vertebral column of *S. acanthias* has an intracentral canal that is open and covered with a velum layer. An open intracentral canal may indicate that the centra are acting as tunics around some sections of a hydrostat, effectively stiffening the vertebral column. These data suggest that the entire vertebral column of sharks, both joints and centra, is mechanically engaged as a dynamic spring during locomotion.

1. Introduction

Biological tissues can, under the right circumstances, function as springs. Springs convert kinetic energy into potential energy; for animals, depending on the behavioral context, this exchange may be used to control body motion or reconfiguration, to smooth or delay delivery of periodic sources of mechanical work, and to combine work from multiple sources (Roberts and Azizi, 2011). If an element of a mechanical system is to act as a spring, it must (i) undergo strain without failure and (ii) possess sufficient stiffness and resilience to store and release mechanical work. In fishes, the axial skeleton has been proposed to act as a spring (Rockwell et al., 1938), with intervertebral joints posited as the structures that strain and act as springs (Home, 1809; Hebrank et al., 1990; Long, 1992, 1995; Schmitz, 1995). However, recent X-ray reconstruction of moving morphology (XROMM) of swimming striped bass, *Morone saxatilis*, has called into question the spring hypothesis, at least for some teleost fishes, since strain of the intervertebral joints never engages the connective tissues to a point where they store significant amounts of mechanical work (see Nowroozi and Brainerd, 2013, 2014). However, even if joints are not storing elastic energy, it is possible that the skeletal elements are. Hence our goal was to test the assumptions of the classic spring hypothesis by measuring the strain in intervertebral joints and the cartilaginous vertebrae of sharks.

We predicted that the axial skeletons of cartilaginous and bony fishes are likely to function differently during swimming for several reasons. First, the cartilaginous vertebrae of elasmobranchs are stronger for a given stiffness than bovine cancellous bone (Porter and Long, 2010; for review, see Summers and Long, 2006). Second, as frequency increases in cyclic bending tests, the elastic

☆ This article is part of a special issue entitled "Axial systems and their actuation: new twists on the ancient body of craniates".

* Corresponding author at: Department of Biological Sciences, Florida Atlantic University, 777 Glades Road, Boca Raton, FL 33431, USA. Tel.: +1 561 297 2188.
E-mail address: me.porter@fau.edu (M.E. Porter).

0944-2006/$ – see front matter © 2013 Elsevier GmbH. All rights reserved.
http://dx.doi.org/10.1016/j.zool.2013.10.007

component of stiffness increases in the vertebral columns of the spiny dogfish, *Squalus acanthias* (Long et al., 2011a), while it decreases in those of the blue marlin, *Makaira nigricans* (Long, 1992). Third, the intervertebral joints of the three elasmobranch fishes that have been tested in bending to date (Long et al., 2011b) lack the neutral zone of bending seen in some bony fishes (see Nowroozi and Brainerd, 2014). Fourth, the vertebral column of elasmobranchs lacks the neural spines, hemal spines, and zygapophyses present in most bony fishes. Finally, we have the obvious difference of material, calcified cartilage versus bone (for review, see Summers and Long, 2006). With material differences in mind, what is particularly intriguing is that sharks have lost the endochondral bone possessed by their ancestors (Smith and Hall, 1990). Thus, if the loss of bone alters or enhances locomotor function of the axial skeleton, then we have uncovered one possible reason for its evolutionary loss.

The short, squat, poorly mineralized vertebrae of most cartilaginous fishes are not well suited to techniques that are usually used to directly measure strain in hard and soft tissues. For in vivo experiments, strain is usually measured in one of three ways. First, tendon force buckles have been surgically implanted on the deep caudal tendons of two species of tuna (*Thunnus albacares* and *Katsuwonus pelamis*) (Knower et al., 1999). Second, the XROMM technique, mentioned above, requires the implantation of radio-opaque markers directly on skeletal elements and restricted external water volume in aquatic species (Nowroozi and Brainerd, 2013). Finally, strain gauges can be glued directly to elements such as an avian m. pectoralis and bony fish cranial elements (Lauder and Lanyon, 1980; Jackson et al., 2011). All of these methods require surgery and each has a set of drawbacks that make them unsatisfactory for our needs. Tendon buckles require a substantial length of elongate, cohesive structure that undergoes tensile loading, but the shark vertebral column has nothing like this. Since X-ray can only penetrate a small volume of water, animals must swim in constricted spaces, making it impossible to study steadily swimming sharks. In our experience, strain gauges do not adhere well to shark skeletal elements because the surfaces weep fluid and are a mosaic of independent tiles. We therefore settled on a strain measuring technique that has been used very successfully for measuring muscle strain: sonomicrometry. Sonomicrometry relies on very small piezoelectric crystals whose position is revealed by the time delay between sending and receiving an ultrasound pulse. Though commonly used in muscle experiments, the very low strain in bone and the ultrasonic reflectivity of this highly mineralized tissue have precluded its use in studies of skeletal strain. The relatively poor mineralization of the shark skeleton should eliminate this last issue.

Biological materials are almost always viscoelastic, and the degree to which strain rate affects performance can vary over a wide range. When considering the possibility of elastic energy storage, it is important but difficult to test the system dynamically using biologically relevant loads. The ideal conditions are in vivo, with as little surgical intervention as possible and with a completely natural behavior in a normal environment. This is a difficult standard to achieve, so a reasonable alternative is to perform some in vivo experiments in a manipulated context and then use ex vivo experiments, physical models and mathematical constructs to ground truth the in vivo work and establish some bounds on the reliability of the data.

We applied this layered approach to understanding vertebral column strain in cartilaginous fishes, with three specific goals in mind: (i) determine the in vivo strain of vertebral centra and intervertebral joints during volitional, unrestrained steady swimming; (ii) measure the strain within and between ex vivo vertebral segments at physiologically relevant deformations; and (iii) explore potential morphological bases for energy storage using histological techniques.

2. Materials and methods

2.1. Histology

Histological sections were taken from a female spiny dogfish, *S. acanthias* (TL = 0.9 m, mass = 3.24 kg) obtained from the Marine Biological Laboratory, Woods Hole, MA specimens collection. The animal was sacrificed with a lethal overdose of tricaine methanesulfonate (MS-222) and the vertebral column was dissected and fixed by immersion in a pH 7.35 buffered solution of 10 ml 10% formaldehyde, 10 ml 25% glutaraldehyde, 20 ml 0.2 M cacodylate buffer and 60 ml PBS (Totland et al., 2011). The vertebral column was decalcified in a solution of formic acid. A scalpel was used to prepare thick sections. The preparation of both transverse and sagittal sections allowed for comprehensive study of the anatomy. We used a pipette to distribute a mixture of methylene blue and toluidine blue stains in aqueous solution to the surface of the thick sections. These stains bind to connective tissue, muscle, and cytoplasm in varying amounts that allow visualization and differentiation. A water rinse was used to remove unfixed stain from the section. Samples were photographed under a light microscope.

2.2. Whole body curvature

To determine whole body curvature of animals ($N = 4$), we recorded volitional swimming in housing tanks at Friday Harbor Laboratories, University of Washington, WA. Video was collected by placing a tripod-mounted camera (Handycam HDR-HC5; Sony Corp., Tokyo, Japan) in a Plexiglas boat on the surface of the water and filming from one meter above. Filming was performed at 30 frames s^{-1} and clips of video (.mov format, 640 × 480 pixels, deinterlaced fields; iMovie HD software; Apple Inc., Cupertino, CA, USA) show an animal swimming along a straight trajectory across the tank. We screened the data to find sequences in which an individual was swimming in a straight line, with steady tail beats, and little acceleration. We analyzed four such steady swimming segments of video, one from each animal, using LoggerPro version 4.0 (Vernier Software & Technology, Beaverton, OR, USA). In each video sequence, seven points on the dorsal midline of the body were manually digitized in each frame of the sequence. The following points were used as major anatomical landmarks: tip of the rostrum, tip of the caudal fin, and the anterior insertions of the first and second dorsal fins. In each frame, these four landmarks were digitized first, and then three points were placed equidistant between two landmarks, for a total of seven landmarks along the dorsal midline.

Curvature (m^{-1}) from five regions along the body was then calculated from the angle of the adjacent segments at each internal (non-terminal) point in the sequence, 2–6. The radius of curvature (m) was estimated, using trigonometry, and its inverse taken to calculate curvature in each of the following regions: region 1 consists of information from points 1 to 3; region 2 from points 2 to 4; region 3 from points 3 to 5; region 4 from points 4 to 6; and region 5 from points 5 to 7. For each individual and each region we sought the maximum curvature, since this value would frame the physiological range of curvatures to use in our ex vivo tests of the vertebral column.

Note that strain data from in vivo experiments were collected from region 5 while ex vivo experiments were performed on the vertebral segments from region 3. While our original intention was to do both types of experiments in region 3, a surgical approach for crystal implantation in this region would have required either a major disruption of the locomotor muscle or full abdominal surgery. Because of our concern for the recovery of the animals and the disruption of the local muscle tissue, we developed, instead, a minimally invasive technique that required we work in region 5 (see Section 2.3 for details). Unfortunately, we were unable to

perform ex vivo tests in the same region, since vertebrae there were small enough that we could not reliably grip the ends of the test segment without slippage. In summary, the measurements of the in vivo and ex vivo strain come from regions 5 and 3, respectively.

To determine if curvature differed among regions, we analyzed data using a one-way ANOVA and Student's *t*-test post hoc comparisons in JMP 8.0 software.

2.3. In vivo strain experiments

We caught adult *S. acanthias* ($N = 5$; four males and one female) by hook and line near-shore fishing at the University of Washington's Friday Harbor Laboratories. Animals ranged in size from 73.5 to 79.0 cm total length and 1.5–1.9 kg. Animals were housed in 2 m diameter tanks supplied with flow-through seawater at a depth of 83 cm.

We anesthetized the animals with 0.3 g MS-222 per liter of seawater. Under anesthesia, three 1 mm sonomicrometry piezoelectric crystals were implanted into the vertebral column, posterior to the second caudal fin using a 15-gauge hypodermic needle allowing us to penetrate the muscle and mineralized tissue with minimal damage (Fig. 1A–C). The surgical site was chosen following several dissections and practice implantations on deceased animals. Crystals were implanted through the vertebral column, entering a centrum dorsolaterally and exiting that same centrum ventrolaterally. In cross-section the angle of the crystral's trajectory was 45° relative to the mid-sagittal plane; this trajectory avoided damage to the spinal cord, spinal nerves, and the intervertebral joint. However, by design the needle did pass through the intervertebral capsule; as shown by in vitro biomechanical tests, disruption of a single intervertebral capsule does not alter the apparent storage or loss moduli of the vertebral column during bending (Long et al., 2011a).

As revealed in post-mortem dissection, this implantation procedure placed the crystal just lateral to the surface of the centrum on the side contralateral to the surgical site. The crystal was held in place by cyanoacrylic tissue cement, which affixed the crystal's leads to the implantation side of the centrum and the skin. While the animal was under anesthesia, we pressed on individual leads while holding the body straight; this allowed an initial test to see if crystals were firmly seated. To reduce motion artifacts caused by the movement of the wires, we stitched and affixed all the leads to the second dorsal fin, leaving some slack between the implantation site and the dorsal fin. For the duration of the experiment, leads where held dorsal to the shark in a way that minimized bending of the sonomicrometry system wires.

Following experiments and euthanasia, we inspected the surgical sites, documented crystal placement with photographs, measured the distance between crystals, calibrated strain at different curvatures, and manually bent the vertebral column to make sure that crystals did not move relative to the centra. Occasionally crystals would have become unseated, moving laterally relative to the centrum during manual bending, and data from these sites were discarded. It is important to reiterate that since the surgery to implant the crystals was done in a minimally invasive procedure without visualization of the implantation site, crystal placement varied among animals.

The benefit of this surgical procedure is that it is minimally invasive, leaving muscle and tissues intact around the area of interest. However, this procedure is limited in several ways. First, because implantation is done by needle, the surgeon must be able to palpate the vertebral column, and to do this accurately requires operating in the caudal region, where there is very little muscle. Second, the placement of the crystals is blind, meaning that we did not know exactly where crystals had been placed until after the experiments were finished and we could perform our post-mortem inspection. Finally, while new techniques should always be viewed cautiously, we note that we have independently validated the most important in vivo result – showing both centra and joints strain – in our ex vivo experiments.

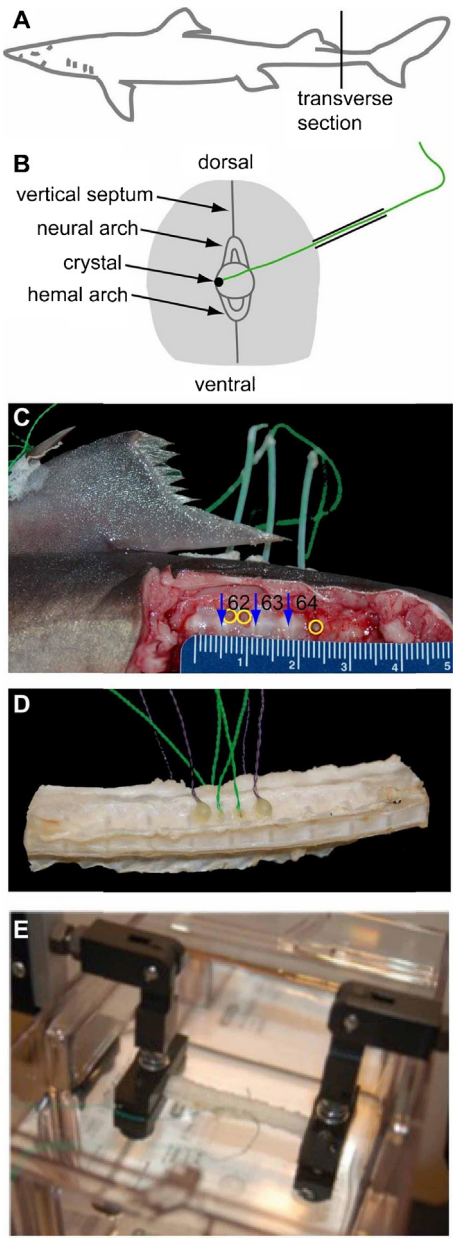

Fig. 1. Vertebral column strain in vivo, in situ, and ex vivo. (A) 1 mm sonomicrometry crystals were implanted into the vertebral column posterior to the second dorsal fin of *Squalus acanthias*. (B) Transverse section of caudal region. Blind surgery was performed, with implantation sites determined by palpating the vertebral column. Sonomicrometry crystals were implanted contralateral to the surgical entry site; thus, the site of implantation and the site of strain measurements were opposite. (C) After in vivo and in situ data collection, the site of implantation was dissected to determine the structures from which strain was measured. Yellow circles denote the location of crystals in this preparation and blue arrows show the intervertebral joints. Centra 62, 63, and 64 are numbered. (D) Vertebral column segment with crystals implanted along the lateral surfaces for ex vivo strain measurements. (E) Vertebral segments were tested in an environmental chamber filled with elasmobranch Ringers solution.

Following surgery, animals recovered in a sea table (22 cm × 60 cm × 120 cm, depth × width × length). While the animal was still under anesthesia, we measured baseline data when the animal's body was straight; we also measured in situ

passive "swimming", by manually creating a traveling wave of bending down the length of the body by gently moving the animal's head left and right in the horizontal plane, and in situ passive "turning," by gently bending the animal's body. After the animal recovered from anesthesia, the in vivo trials began; the animal swam in the tank, and these volitional movement data were recorded during movement across the tank consisting of 2–5 tail beats. We also recorded turning movements and intermittent movements of the tail.

Sonomicrometry data were collected using a TRX 8 Sonometrics Digital Ultrasonic Measurement System (Sonometrics Corp., London, ON, Canada) and the following software packages: Sonolab v. 5.40.0J and SonoSoft v. 3.4.27-RC4 (Sonometrics Corp., London, ON, Canada). The transmit pulse was the parameter controlling the length of the ultrasound pulse, 218.8 ns, applied to the transmitting crystal. We used a sampling rate, the inverse of the time taken for any single transmitter to fire an ultrasound signal, of 292.57 Hz. We set the inhibit delay, the difference between the electrical and the ultrasound signal, to 1.0 mm. For each trial, we calculated the maximum (tension) and minimum (compression) strain values. As these values are generally symmetrical, we report only the maximum values for strain. For each shark, a suite of behaviors was captured, as mentioned above; these data were analyzed using ANOVA with Student's *t*-test post hoc comparisons in JMP 8.0 software.

2.4. Ex vivo strain experiments

We used separate ex vivo measurements, on different individuals of *S. ancanthias*, to validate our in vivo results. Based on ex vivo compression tests of individual centra from various species, we predicted that there would be strain in centra (Porter et al., 2006; Porter and Long, 2010). We used vertebral columns dissected from six individuals, ranging in size from 77 to 87 cm total length; four were males. Vertebral columns were frozen and stored prior to use. Segments of ten centra and nine intervertebral joints were dissected from the precaudal region of each column ventral to the first dorsal fin (Fig. 1D and E). Segments were approximately 1/7 of the length of the entire precaudal column.

We used an eight-channel, digital sonomicrometer, described above in Section 2.3. This system was used to measure strain in the intervertebral joints and centra ex vivo as a Titron 250 materials testing system (MTS; MTS Systems, Eden Prairie, MN, USA) imposed dynamic bending loads measured by a calibrated 25 N load cell. To measure strain at the joint and centra, eight sonometric crystals were affixed along the lateral surfaces of a motion segment (two centra separated by an intervertebral joint) using cyanoacrylate glue (Super Glue Gel; Elmer's Products Inc., Columbus, OH, USA). We placed 1 mm crystals around the joint and 2 mm crystals at the edges of the adjacent centra. Once the glue had set, crystals were manually tested to make sure that they were firmly affixed.

Segment preparations were immersed in an environmental chamber containing room temperature elasmobranch Ringers solution (Forster et al., 1972) to maintain tissue hydration and allow the sonomicrometry crystals to communicate. Each segment was clamped into a rig that applied bending couples to both ends of the segment (Long et al., 2011b). We varied the linear actuator amplitudes (5, 10, 15 mm) and sinusoidal oscillation frequencies (0.25, 0.5, 1.0 Hz). Based on the amplitude settings from the MTS and the geometry of our rig and column segment, we calculated the maximum curvature for each segment (Long et al., 2011b). Taking bilateral strain measurements allowed for the separation of pure bending strains, which are laterally equal and opposite, from symmetric axial strain.

We used structure (centrum, joint, and motion segment), frequency (Hz), and curvature (m^{-1}) as the three main effects in a full factorial statistical model using JMP 8.0 software (SAS Institute, Cary, NC, USA). We included shark total length (m) as a covariate to account for differences among animals.

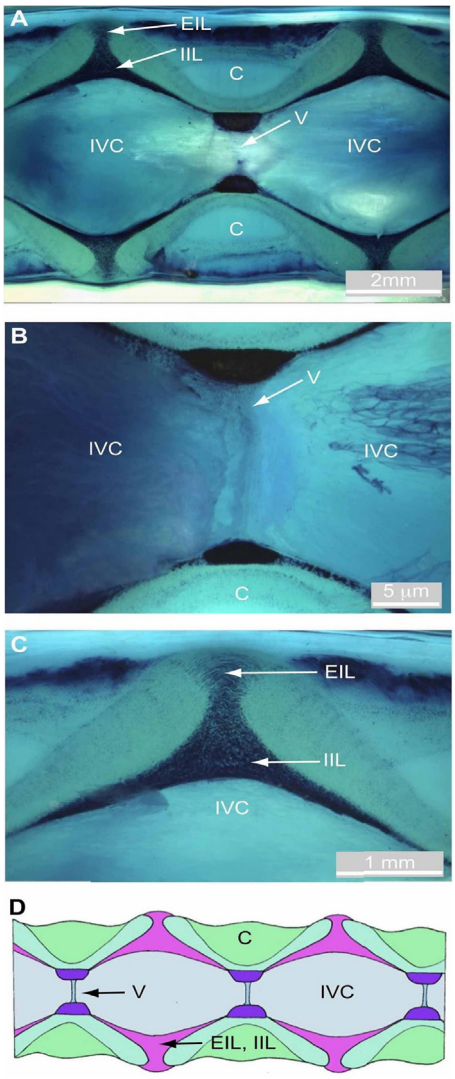

Fig. 2. Morphology of *Squalus acanthias* vertebral column. (A) Sagittal section showing two intervertebral capsules separated by a thin velum. (B) The velum separates the two intervertebral joint capsules. (C) The internal and external intervertebral ligaments encapsulate the intervertebral joint. (D) Schematic showing the intervertebral joint capsules separated by the velum. This may indicate that each joint capsule is operating as an independent hydrostat during bending. Tissues in (A)–(C) were stained with a mixture of methylene blue and toluidine blue. Abbreviations: C, centrum; EIL, external intervertebral ligament; ILL, internal intervertebral ligament; IVC, intervertebral capsule; V, velum.

3. Results

3.1. Morphology of the intervertebral joint and capsule

S. acanthias centra are composed of a double cone of mineralized cartilage (Fig. 2A). Sagittal sections show the intervertebral capsule is partitioned by a thin velum of approximately 1 µm thickness occurring in the intracentral canal (Fig. 2B). Based on differential staining, the velum appears to be composed of several layers. The intervertebral capsule is bounded laterally by the external and internal intervertebral ligaments (Fig. 2C). The external intervertebral ligaments are composed of distinct layers that appear to be interdigitated with the unstained cartilaginous matrix that forms the opposing rims of the centra. In contrast, the internal intervertebral ligaments lack clear layers and interdigitation with the centra.

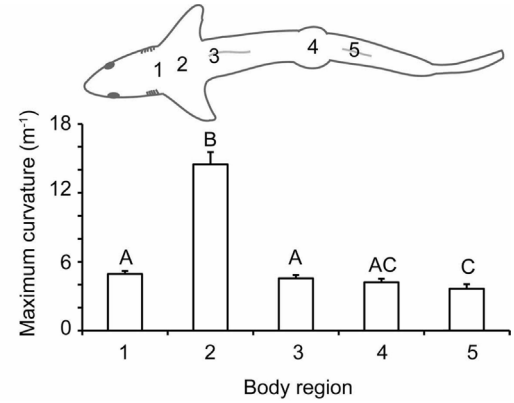

Fig. 3. Curvature of the dorsal midline during steady free-swimming in *Squalus acanthias*. Curvature varies by region ($F_{4,15}$ = 266.5; P < 0.0001). The in vivo strain experiments were conducted in region 5. The ex vivo strain experiments were conducted on vertebral segments from region 3, which experiences mean maximal curvatures during steady swimming of 4.55 m^{-1}, a maximum that was matched in the ex vivo experiments. The five body regions are shown on the dorsal outline of the shark. Kinematic data were taken from different video clips, one from each animal (N = 4). Different letters above bars denote significant differences among groups.

Taken together, both external and internal intervertebral ligaments form a continuous cylinder of tissue that alternates from a lateral position at the joints to a medial position near the velum (Fig. 2D).

3.2. Whole-body curvature during swimming

Mean maximum curvature (m^{-1}) of the body's midline varies along the length of the *S. acanthias* during swimming ($F_{4,15}$ = 266.5; P < 0.0001; Fig. 3). Region 2, in the pre-caudal column between the pectoral fins, has the greatest curvature, nearly four times greater than that of region 5. Data from in vivo experiments were collected from region 5 while ex vivo experiments were collected from region 3 (see Section 2.2 for explanation). Note that while the maximum curvature is greater in region 3 than 5, the magnitude of the difference is smaller than either difference compared to region 2, with mean maximum curvatures of 4.5 and 3.6 m^{-1}, respectively, for regions 3 and 5. Curvatures imposed on vertebral segments from region 3 during ex vivo experiments are within the physiological range seen in steadily swimming *S. acanthias*. Since we did not measure the curvature of the midline during the in vivo strain experiments, we assume that the values measured here for region 5 are first approximations for curvature when strain was measured during volitional steady swimming (see Section 3.3).

3.3. In vivo strain experiments

As a shark swam, tensile and compressive strains occurred in the centra (Fig. 4A). These low-magnitude strains, reaching 2% at their maximum between crystals implanted in the same centrum, were rhythmic and mirrored the steadily traveling wave of bending that deformed the caudal region of the body. When strain was measured between crystals located on different but adjacent centra, we saw the same pattern of strain in the centrum as in the centrum and intervertebral joint (but note the higher strain in the segments; Fig. 4B). When this same individual, post-mortem, was manually undulated, both the pattern and magnitudes of both types of strain were similar (Fig. 4C).

Because our surgical technique was minimally invasive (see Section 2.3), we were unable to create identical preparations in each shark. Individuals 1 and 3, for example, were the only ones with strain measured within a single centrum. Hence we report results summarized by individual (Fig. 5). Strain (%) varied depending on the specific movement behavior of the shark in three of the

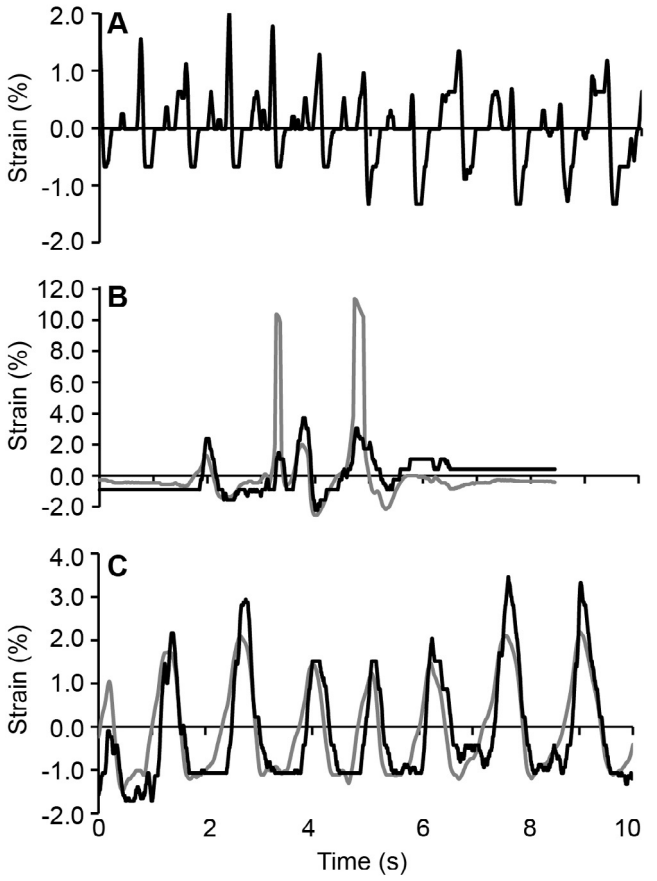

Fig. 4. In vivo and in situ sonomicrometry traces. (A) Steady undulation in vivo. In this trace the shark was moving with steady undulations at approximately 1 Hz. Centrum strain was 1–2%. (B) Intermittent undulation in vivo. This trace shows the strain of the vertebral segment (gray) and the centrum (black). (C) Manual undulation in situ. After a lethal overdose of MS-222, the shark body was manually undulated. While the traces from (A) and (B) were under active control of the shark, this in situ trace shows passive vertebral column strain. In all panels, black traces are from the crystal pair in the centrum while gray traces show the vertebral segment (three centra and two intervertebral joints). Negative values indicate compression and positive values, tension.

four individuals. In individual 1, centrum strain varied by behavior (P = 0.025) and strain produced during in situ turns was nearly double that produced in other behaviors (Fig. 5A). In individual 2, there was no difference (P = 0.081) in strain among behaviors in a centrum–joint–centrum motion segment (Fig. 5B). However, there were differences in a two-joint motion segment (P = 0.001) with the largest strains occurring during in situ swimming motions and during in vivo volitional movements. In individual 3, as in individual 1, centrum strain was significantly greater during in situ turning (P = 0.008), nearly double the strain seen during other behaviors (Fig. 5C). In individual 4, we found no significant difference among behaviors in strains measured in a centrum–joint–centrum motion segment (P > 0.05; Fig. 5D).

3.4. Ex vivo strain experiments

Under the controlled and repeatable conditions of the ex vivo experiments on isolated segments of vertebral columns, strain could be measured directly in the centrum and in the intervertebral joint. As with the in vitro experiments, strain from different individuals varied (Fig. 6). Under identical bending frequency (1 Hz) and similar curvatures, the patterns in strains at centrum and joint varied from identical (individual 2, Fig. 6A) to higher strain in the

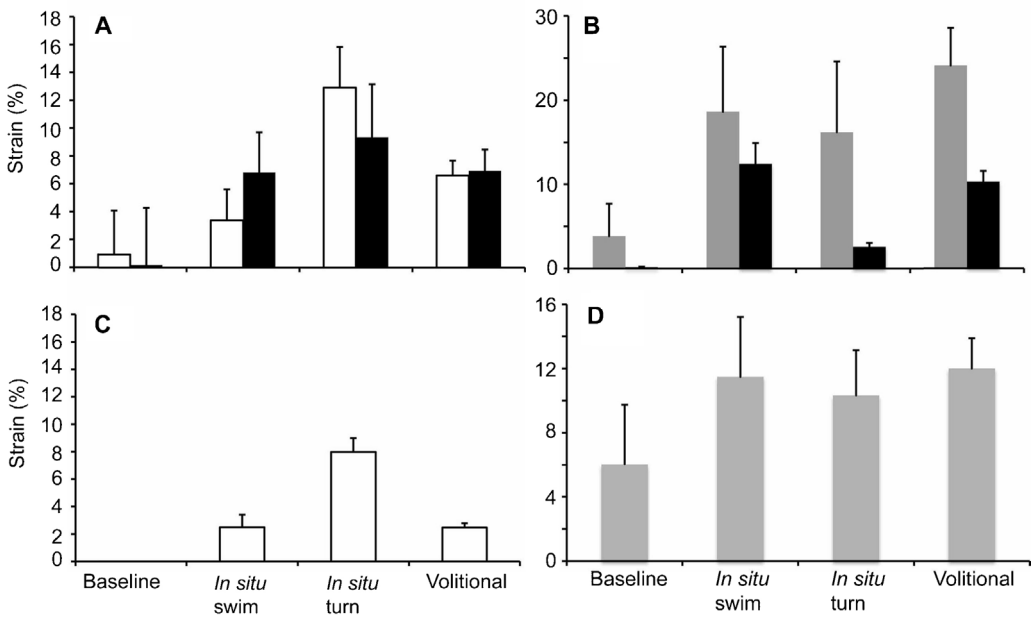

Fig. 5. In vivo and in situ strain in the vertebral column of four *Squalus acanthias* individuals. (A) In individual 1, strain changes in a single centrum significantly with behavior ($F_{3,74} = 3.29$; $P = 0.0252$), while it does not change significantly in a three-centrum–two-joint motion segment. Centrum strain was greatest in situ, with the experimenter turning the animal while it was anaesthetized. (B) In individual 2, strain changes with behavior in a centrum–joint–centrum motion segment ($P = 0.081$). Strain changes significantly with behavior in a three-centrum–two-joint motion segment ($F_{3,56} = 5.97$; $P = 0.0013$) where in situ swimming and in vivo volitional movements produce the largest vertebral column changes. (C) In individual 3, centrum strain varies significantly with behavior ($F_{2,59} = 8.1384$; $P = 0.008$), with the largest strains being produced during in situ turning. (D) In individual 4, there were no significant differences among behaviors. For all panels, the colors (white, gray, black) indicate strain in a centrum (white bars), a centrum–joint–centrum segment (gray bars), and a three-centrum–two-joint segment (black bars).

centrum (individual 1, Fig. 6B) to higher strain in the joint (individual 6, Fig. 6C).

Ex vivo strain at the centrum, intervertebral joint, and motion segment (two centra and their shared joint) changes significantly with changes in dynamic bending ($F_{12,134} = 3.94$; $P < 0.0001$; Table 1). The main effects of the model (frequency, structure, and curvature) were all significant ($P = 0.0004$, 0.0149, and 0.0004; respectively). The only interaction that was significant was frequency × curvature ($P = 0.0078$): the strain at 1.0 Hz increases faster, on average across all three structure types, with increasing curvature than it does at either 0.5 or 0.25 Hz (Fig. 7). Shark total length, as a covariate, was not significant. Centrum, joint, and motion segment strain all varied with increasing changes in frequency (model scaled estimates; Fig. 7 and Table 1).

4. Discussion

For sharks, the concept that the vertebral column is a series of rigid elements and flexible hinges is inaccurate. Both the vertebral centra and intervertebral joints of spiny dogfish sharks, *S. acanthias*, undergo strain during swimming (Figs. 4 and 5). Both also strain when isolated segments of vertebral column are tested during mechanical bending (Figs. 6 and 7). Finally, the magnitude of ex vivo strain in the centra may be, at times and in only some individuals, higher than that of the adjacent intervertebral joints (Fig. 6). In sum, our data refute the hypothesis that strain of the vertebral column in lateral bending is limited to the intervertebral joints.

What are the functional consequences of strain in the centra? Consider that the mechanical work in, W_i (Nm), to bend the vertebral column is proportional to the product of the flexural stiffness, EI (N m^2), the square of the curvature, κ^2 (m^{-2}), and the length of the column that undergoes strain, l (m). The work out, W_o, also known as the elastic recoil, is the product of W_i and the resilience, R (%) (Long et al., 2011a,b). All else being equal, the elastic recoil is proportional to l, which increases dramatically with the engagement of the straining centra in the spring. For example, if joints account for roughly 16% of the axial length of the column (1.01 mm and 6.34 mm for average joint and centrum lengths anterior to the caudal peduncle, respectively, from measurements on five *S. acanthias* in this study), then the engagement of centra as a spring increases the mechanical work stored and released by a factor of six. While this is a rough approximation, the point is clear: sharks are built for speed.

How much work or elastic recoil (W_o) is available during swimming? We use the values of mechanical properties measured from dynamically bending *S. acanthias* vertebral columns where the average apparent elastic modulus, E', is 1.1 MPa at a physiological curvature of 4 m^{-1} and a bending frequency of 1.0 Hz (Long et al., 2011a,b). The average resilience R is 0.67, where $R = 1/e^{\pi \tan \delta}$; $\tan \delta$ is the ratio of E'', the apparent loss modulus, and E', where E'' is 0.14 MPa and is measured at the same curvature and frequency as E'. The average length l of the vertebral column from the head to the caudal peduncle is 57.62 cm ($n = 5$, *S. acanthias*, from this study). The average second moment of area, I, is 1.626×10^{-9} m^4, from the average diameter of all of the centra anterior to the peduncle, 6.75 mm ($n = 5$, *S. acanthias*), where $I = (\pi/4)r^4$. With these values, we calculate $W_i = 16.48$ mJ and $W_o = 11.05$ mJ.

What is the biological relevance of these values, or how does a W_o of 11.05 mJ figure into the energy budget of *S. acanthias*? For *S. acanthias*, metabolic rates at 10 °C are on average 32.4 and 49.2 mg O_2/kg h for resting and routine swimming movements in a circular tank (Brett and Blackburn, 1978). The difference is the metabolic cost of routine swimming behaviors, 16.8 mg O_2/kg h or 33.6 mg O_2/h for a 2 kg animal. We convert the oxygen consumption to calories using the factor of 4.8 kcal per liter of O_2; that value is then converted to Joules per second to yield power in Watts (W). The metabolic power cost, P_m, of routine swimming in *S. acanthias* is thus 0.1874 W. For swimming with a tail beat frequency of 1.0 Hz, a shark would bend and unbend its vertebral column twice in a second, hence the power input, P_i, required to bend the vertebral

Table 1
Statistical models for ex vivo strain during vertebral segment bending.

Effects test		Scaled estimates	
	P value	Term	Scaled estimates
Main effects			
Frequency (Hz)	0.0004	Intercept	0.0082083
Curvature (m^{-1})	0.0004	Structure [centra]	0.0051757
Structure	0.0149	Structure [joint]	−0.001179
		Structure [ms]	−0.003996
Interactions		Frequency (Hz)	0.0045797
Frequency × curvature	0.0078	Structure [centra] × frequency	0.0047401
Frequency × structure	0.0933	Structure [joint] × frequency	−0.002188
Curvature × structure	0.1267	Structure [ms] × frequency	−0.002552
Frequency × curvature × structure	0.1937	Curvature (m^{-1})	0.0061842
		Structure [centra] × curvature	0.0056161
Covariate		Structure [joint] × curvature	−0.002001
Shark TL (m)	0.1134	Structure [ms] × curvature	−0.003615
		Frequency × curvature	0.0045086
		Structure [centra] × frequency × curvature	0.0060295
		Structure [joint] × frequency × curvature	−0.002455
		Structure [ms] × frequency × curvature	−0.003575
		Shark TL (m)	0.0032282

ms, motion segment; TL, total length.

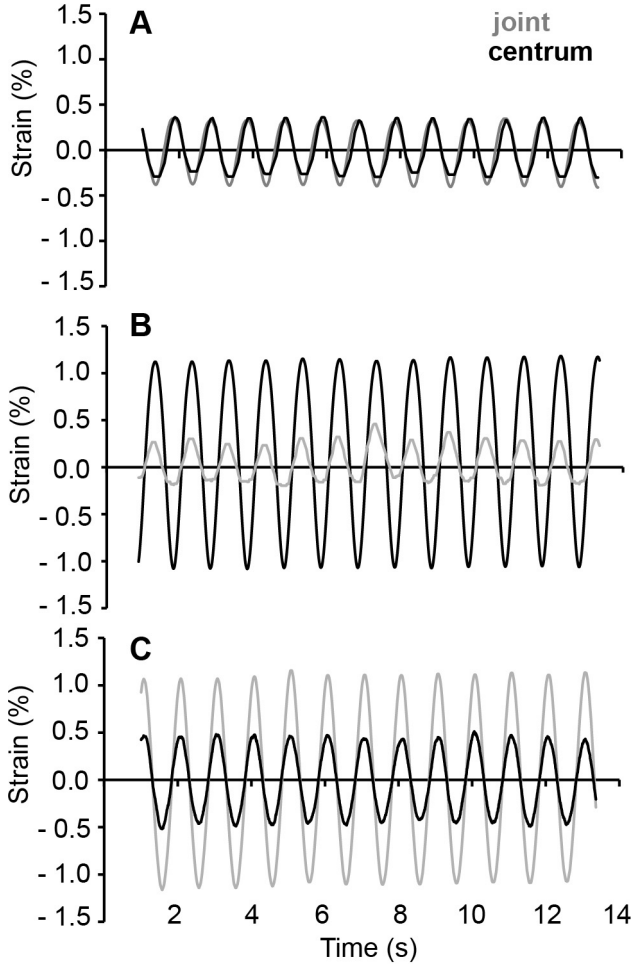

Fig. 6. Representative ex vivo strain in vertebral column segments of three *Squalus acanthias*. Segments were bent sinusoidally at 1.0 Hz and 10 mm MTS amplitude. (A) In some instances, the strains in the joins (gray) and in the centrum (black) were similar in the same segment. (B) In some cases, the centrum strain was greater than the strain in the joint in the same segment. (C) In other cases, joint strain was larger than centrum strain in the same segment.

column is twice W_i, or $P_i = 0.0330$ W; the ratio of P_i and P_m is 0.176. Thus, from our data, we estimate that about 18% of the P_m is used to power the bending of the vertebral column. But some of that P_m is returned in recoil output power, P_o, twice W_o or $P_o = 0.022$ W. Hence the proportion of P_o to P_m is 0.117; thus about 12% of P_m is returned as recoil power. The difference between P_i and P_o as a proportion of P_m is 0.0580, thus the power that is lost in bending the vertebral column is about 6% of P_m.

Since a shark expends 6% of its metabolic power to bend the vertebral column, then what, if anything, is its return on investment for the backbone functioning as a spring? In other words, what useful mechanical work is being done by the recoil of the spring? Undulatory swimming is characterized by a traveling wave of body bending that moves from head to tail. We know from electromyographic studies in a wide variety of elasmobranch species that this traveling wave of bending is associated with a traveling wave of muscle activity (Shadwick and Gemballa, 2006). Since the segmental muscles generate moment locally, bending the body and the vertebral column to the ipsilateral side, we propose that the recoil of the vertebral column locally helps augment contracting muscle on the contralateral side that is acting to straighten the vertebral column. When viewed from the perspective of the entire traveling wave of bending, the local *straightening of the body powered by elastic recoil of the vertebral column propagates the body bends caudally*. For sharks, a 6% metabolic power investment in bending their vertebral column is the price they pay for the mechanical recoil power to make undulatory waves.

The vertebral structures that likely store and return elastic energy can be examined in histological sections (Fig. 2). The arrangement and relative sizes of these structures offer insight into how important they are likely to be in terms of bearing the strains measured in this study. First of all, the robust external and internal intervertebral ligaments link the rims of adjacent centra (Fig. 2; Symmons, 1979). If the neutral axis of bending runs through the mid-sagittal plane of the joint, then these connective tissues are located in the most lateral position and will, therefore, be subjected to the most strain of any of the joint tissues. Second, we propose that the external intervertebral ligaments bear the tensile loads while the internal intervertebral ligaments bear the compressive loads. Axially oriented fibers of the external intervertebral ligaments are clearly present, suggesting a morphology built for tensile loading, while the unoriented fibers of the internal intervertebral ligaments would be in a position to take compressive loads. The presence of

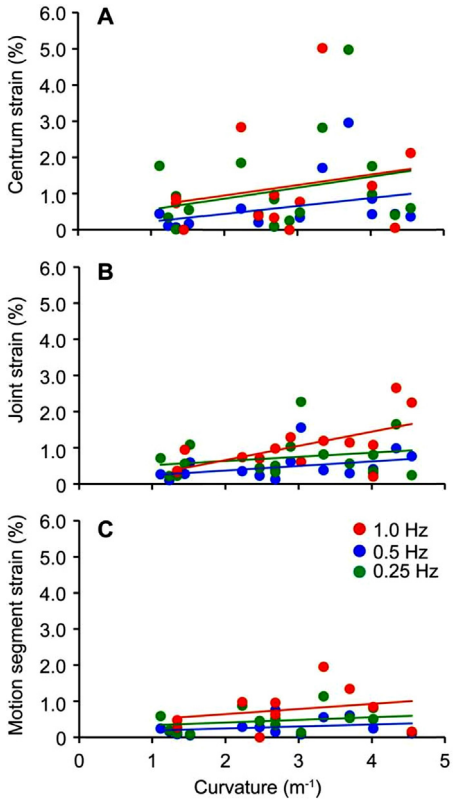

Fig. 7. Ex vivo strain of bending vertebral columns of *Squalus acanthias*. Segments from six sharks were bent at three frequencies (0.25, 0.5, and 1.0 Hz) and varying curvatures (m^{-1}) produced by 5, 10, and 15 mm displacements on the MTS (Table 1). In the whole model, frequency ($P = 0.0004$), curvature ($P = 0.0004$), and structure ($P = 0.0149$) are all significant effects. (A) Centrum strain increased with increasing curvature and frequency. (B) Joint strain increased with both increasing frequency and curvature. (C) Motion segment strain increased with curvature and frequency.

clear interdigitation of the external intervertebral ligaments with the matrix of the rims also supports the idea of tensile load-bearing for these fibers.

The vertebral centra are built of calcified cartilage that forms hourglass-shaped cylinders. In section, the lateral walls of these cylinders appear as curved bars (Fig. 2). In three dimensions, this hourglass shape is biconic, with the tapered ends of the right-circular cones intersecting to form the patent intervertebral canal. As a single structural unit, each centrum is shaped as a three-dimensional leaf spring. By virtue of its biconic shape, the centrum can store energy in tension, by straightening its curved surface, and in compression, by increasing the curvature of its surface. Compression tests of isolated centra from eight elasmobranch species show that these biconic skeletal elements can sustain mean strains of 12% before yielding (Porter et al., 2006; Porter and Long, 2010). This yield strain is greater than any strain we report for compression in *S. acanthias* (but note the occasional tensile strain near 12%, Fig. 4). In summary, we propose that the centra function as biconic, biphasic (tension and compression) springs.

Medial to the conic walls of the centra and the intervertebral ligaments we see an amphicoelous capsule structure that is largely devoid of fibrous tissue (Fig. 2A). Present inside this intervertebral capsule is a weak colloidal gel along with vacuolated cells of the notochord. Hydrostatic pressures above ambient pressure have been measured in notochords of adult white sturgeon, *Acipenser transmontanus* (Long, 1995) and manipulated osmotically in adult hagfish, *Myxine glutinosa* (Sinwell et al., 1999). Home (1809) reported the expulsion of gel from the intervertebral capsule of a beached basking shark. During our own dissections of fresh vertebral columns, we have seen similar expulsions but have yet to develop an experimental technique to allow accurate pressure measurements inside the capsule. In addition, the material properties of the colloidal gel in the intervertebral capsule have yet to be determined. When we punctured three intervertebral capsules of ex vivo vertebral column segments of *S. acanthias*, we found that their elastic properties during bending were unchanged; however, their viscous properties, measured by the loss modulus, increased (Long et al., 2011b). While these various results support the hypothesis that hydrostatic pressure of the intervertebral capsule affects joint strain and movement (Schmitz, 1995), the exact nature of the relationships between morphology and pressure remain unclear in intervertebral joints.

Considering the intervertebral capsule of *S. acanthias* as a hydrostatic system, we find the morphology intriguing (Fig. 2). Each centrum has a sizeable medial canal that, in this species, is covered by a velum of connective tissue. The presence of a velum prevents the gel under pressure from moving into adjacent intervertebral capsules. Hence, we predict that the intervertebral capsules are independent hydrostatic chambers, allowing locally generated pressure changes to impact only the local tissues of that joint and the joint's centra. We note that the transfer of stress from one centrum to another via hydrostatic pressure likely occurs in a very different way than the transfer of stress via the fibers of the intervertebral ligaments. Hydrostatic pressure is an omnidirectional stress field while stress in fibers is likely to be highly directional.

5. Conclusions

In cartilaginous fishes, we have two independent lines of evidence that both intervertebral joints and vertebral centra undergo strain when the axial skeleton bends during swimming. Thus, at least in this group of fishes, a vertebral column cannot be thought of as an alternating series of rigid (vertebrae) and flexible (joints) elements. Instead the whole column strains during bending. Combined with data on the mechanical properties of the bending column (Long et al., 2011b), the functional consequence of this finding is clear: the whole axial skeleton of sharks operates as a spring during locomotion. We propose that this mechanical function is made possible by two sets of intervertebral ligaments, one set resisting tension and the other resisting compression, and centra that operate as biconic, biphasic (tension and compression) springs.

Finally, the presented experiments on sharks may offer an insight into an evolutionary puzzle. Since bone is the ancestral state of the skeleton of all jawed vertebrates, why did elasmobranchs lose bone? We propose that the loss of bone was driven, in part, by selection for enhanced spring behavior of the axial skeleton. We are struck by the difference between how cartilaginous and bony fishes may have converged on the same mechanical solution. Whereas cartilaginous fishes lost bone and thus engage their vertebral centra as springs, bony fishes do not. Instead, in some bony fishes we see the extra-central bony elements – neural arches, hemal arches, and zygapophyses – arranged to cross the axis of the joint, bend, and store energy (for review and new experiments, see Ashley-Ross et al., 2014).

In both cartilaginous and bony fishes, it is worth keeping in mind that we see variation in mechanical behavior and functional morphology of the axial skeleton within individuals, between individuals, and among species. Thus, while the axial skeletons of some bony fishes lack the capacity to function as springs, others do not (for review, see Nowroozi and Brainerd, 2014). To fully understand the many different kinds of locomotor functions embodied by the axial skeleton in different vertebrates, we clearly need additional studies and new approaches, such as we have developed here, to investigate more species.

Acknowledgements

We thank Carl Bertsche from Vassar's Science Technology Support Department for his valuable assistance in the design and engineering of our dynamic-bending and compression rigs, and Harald Kryvi and Ger Totland at Bergen University for their assistance with histological preparations. Two anonymous reviewers improved this manuscript with their constructive comments. This work was supported by NSF grants (IOS-0922605 to J.H.L. and M.E.P. and IOS-1256602 to A.P.S.). Undergraduate funding to C.D. and J.J.S was provided by the Vassar Undergraduate Summer Research Institute. Sonometrics Corp. provided technical support.

References

Ashley-Ross, M.A., Perlman, B.M., Gibb, A.C., Long Jr., J.H., 2014. Jumping sans legs: does elastic energy storage by the vertebral column power terrestrial jumps in bony fishes? Zoology 117, 7–18.

Brett, J.R., Blackburn, J.M., 1978. Metabolic rate and energy expenditure of the spiny dogfish, *Squalus acanthias*. J. Fish. Res. Board Can. 35, 816–821.

Forster, R.P., Goldstein, L., Rosen, J.K., 1972. Intrarenal control of urea reabsorption by renal tubules of the marine elasmobranch, *Squalus acanthias*. Comp. Biochem. Physiol. 42A, 3–12.

Hebrank, J.H., Hebrank, M.R., Long Jr., J.H., Block, B.A., Wainwright, S.A., 1990. Backbone mechanics of the blue marlin *Makaira nigricans* (Pisces, Istiophoridae). J. Exp. Biol. 148, 449–459.

Home, E., 1809. On the nature of the intervertebral substance in fish and quadrupeds. Proc. R. Soc. Lond. 16, 177–187.

Jackson, B.E., Tobalske, B.W., Dial, K.P., 2011. The broad range of contractile behaviour of the avian pectoralis: functional and evolutionary implications. J. Exp. Biol. 214, 2354–2361.

Knower, T.R., Shadwick, E., Katz, S.L., Graham, J.B., Wardle, C.S., 1999. Red muscle activation patterns in yellowfin (*Thunnus albacares*) and skipjack (*Katsuwonus pelamis*) tuna during steady swimming. J. Exp. Biol. 202, 2127–2138.

Lauder, G.V., Lanyon, L.E., 1980. Function anatomy of feeding in the bluegill sunfish, *Lepomis macrochirus*: in vivo measurements of bone strain. J. Exp. Biol. 84, 33–55.

Long Jr., J.H., 1992. Stiffness and damping forces in the intervertebral joints of blue marlin, (*Makaira nigricans*). J. Exp. Biol. 162, 131–155.

Long Jr., J.H., 1995. Morphology, mechanics, and locomotion: the relation between the notochord and swimming motions in sturgeon. Environ. Biol. Fishes 44, 199–211.

Long Jr., J.H., Koob, T., Schaefer, J., Summers, A., Bantilan, K., Grotmol, S., Porter, M.E., 2011a. Inspired by sharks: a biomimetic skeleton for the flapping, propulsive tail of an aquatic robot. Mar. Technol. Soc. J. 45, 119–129.

Long Jr., J.H., Krenitsky, N., Roberts, S.F., Hirokawa, J., deLeeuw, J., Porter, M.E., 2011b. Testing biomimetic structures in bioinspired robots. Int. Comp. Biol. 51, 158–175.

Nowroozi, B.N., Brainerd, E.L., 2013. X-ray motion analysis of the vertebral column during the startle response in striped bass, *Morone saxatilis*. J. Exp. Biol. 216, 2833–2842.

Nowroozi, B.N., Brainerd, E.L., 2014. Importance of mechanics and kinematics in determining the stiffness contribution of the vertebral column during body-caudal-fin swimming in fishes. Zoology 117, 28–35.

Porter, M.E., Long Jr., J.H., 2010. Vertebrae in compression: mechanical behavior of arches and centra in the gray smooth-hound (*Mustelus californicus*). J. Morphol. 271, 366–375.

Porter, M.E., Beltrán, J.L., Koob, T.J., Summers, A.P., 2006. Material properties and biochemical composition of mineralized vertebral cartilage in seven elasmobranch species (Chondrichthyes). J. Exp. Biol. 209, 2920–2928.

Roberts, T.J., Azizi, E., 2011. Flexible mechanisms: the diverse roles of biological springs in vertebrate movement. J. Exp. Biol. 214, 353–361.

Rockwell, H., Evans, F.G., Pheasant, H.C., 1938. The comparative morphology of the vertebrate spinal column: its form as related to function. J. Morphol. 63, 87–117.

Schmitz, R.J., 1995. Ultrastructure and function of cellular components of the intercentral joint in the percoid vertebral column. J. Morphol. 226, 1–24.

Shadwick, R.E., Gemballa, S., 2006. Structure, kinematics, and muscle dynamics in undulatory swimming. Fish Physiol. 23, 241–280.

Sinwell, B.J., Czuwala, P.J., Long Jr., J.H., Koob-Emunds, M., Koob, T.J., 1999. Bending mechanics of the hagfish (*Myxine glutinosa*) notochord under different osmotic treatments. Bull. MDIBL 38, 94–96.

Smith, M.M., Hall, B.K., 1990. Development and evolutionary origins of vertebrate skeletogenic and odontogenic tissues. Biol. Rev. 65, 277–373.

Summers, A.P., Long Jr., J.H., 2006. Skin and bones, sinew and gristle: the mechanical behavior of fish skeletal tissues. In: Shadwick, R.E., Lauder, G.V. (Eds.), Fish Biomechanics. Academic Press, San Diego, pp. 141–177.

Symmons, S., 1979. Notochordal and elastic components of the axial skeleton of fishes and their functions in locomotion. J. Zool. 189, 157–206.

Totland, G., Fjelldal, P., Kryvi, H., Løkka, G., Wargelius, A., Sagstad, A., Hansen, T., Grotmol, S., 2011. Sustained swimming increases the mineral content and osteocyte density of salmon vertebral bone. J. Anat. 219, 490–501.